Journal of Engineering Science and Technology
Vol. 3, No. 3 (2008) 213 - 223

NUMERICAL MODELING AND DYNAMIC SIMULATIONS OF NONLINEAR AEROTHERMOELASTIC OF A DOUBLE-WEDGE LIFTING SURFACE

ARIF A. EBRAHEEM AL-QASSAR

University of Technology, Control and Systems Engineering Department
35010, Baghdad, Iraq
Email: arifqassar@yahoo.com

Abstract

The design of the re-entry space vehicles and high-speed aircrafts requires special attention to the nonlinear thermoelastic and aerodynamic instabilities of their structural components. The thermal effects are important since temperature environment influences significantly the static and dynamic behaviors of flight structures in supersonic/hypersonic regimes. To contribute to the understanding of dynamic behavior of these "hot" structures, a double-wedge lifting surface with combined freeplay and cubic stiffening structural nonlinearities in both plunging and pitching degrees-of-freedom operating in supersonic/hypersonic flight speed regimes has been analyzed. A third order Piston Theory Aerodynamics is used to evaluate the applied nonlinear unsteady aerodynamic loads. The loss of torsional stiffness that may be incurred by lifting surfaces subjected to axial stresses induced by aerodynamic heating is also considered. The aerodynamic heating effect is estimated based on the adiabatic wall temperature due to high speed airstreams. Modelling issues as well as simulation results have been presented and pertinent conclusions outlined. It is highlighted that a serious loss of torsional stiffness may induce the dynamic instability of the lifting surfaces. The influence of various parameters such as flight condition, thickness ratio, freeplays and pitching stiffness nonlinearity are also discussed.

Keywords: Nonlinear aerothermoelastic analysis, Thermal loading, Freeplay, Hypersonic speed.

1. Introduction

Strong interactions can occur between high speed flow field and the aerospace structural components, such as wings and empennages, resulting in several

important aeroelastic phenomena. These aeroelastic phenomena can dramatically influence the performance of the flight vehicle. Moreover, the tendency to reduce weight, increase structural flexibility and operating speed, certainly increase the likelihood of the flutter occurrence within the vehicle operational envelope [1-7]. However, aerospace systems inherently contain complex interactions of structural and aerodynamic nonlinearities [8]. These complex aeroelastic interactions may be so dangerous to worsen the performance of the flight vehicle because an aeroelastic system may exhibit a variety of responses that are typically associated with nonlinear regimes of response, including Limit Cycle Oscillations (LCO), flutter, and even chaotic vibrations [9].

Aerodynamic nonlinearities are such as complex nonlinear flows with shock waves, vortices, flow separation in case of high angle of attack and aerodynamic heating. Structural nonlinearities can be subdivided into distributed nonlinearities and concentrated nonlinearities. Distributed nonlinearities are spread over the entire structure-formed material and geometric nonlinearity, while concentrated nonlinearities have local effects on a control mechanism or an attachment of external stores. Most of flight vehicles including generic missile, space shuttle and high-performance combat aircraft may have inherently concentrated structural nonlinearities such as freeplay, friction, hysteresis and preloads in the hinge part of their control surfaces and folded sections, etc. Concentrated structural nonlinearities may stem from a worn or loose hinge connection of control surfaces, joint slippages, and manufacturing tolerances. Concentrated structural nonlinearities are generally known to cause significant instability in the aeroelastic responses of aero-surfaces. Among all these several nonlinearities, the freeplay usually gives birth to the most critical flutter condition [10]. Control surface freeplay must be removed to increase the linearity of the measured data. Another example of the detrimental effects is the aerothermoelastic loads that play a key role in the design of the aero-surfaces of the supersonic/hypersonic aerospace vehicles and re-entry vehicles. Kinetic heating at high Mach numbers can seriously reduce structural stiffness. Depending on the temperature and initial conditions, the nonlinearities belong to hardening or softening spring type. The strength of metal is reduced by its exposure to a high-temperature for a period of time.

In the present paper a two-degree-of-freedom (2-DOF) airfoil system (typical section model) can provide many practical insights and useful information about the physical aeroelastic phenomena [11]. The nature of the LCO, which provides important information on the behavior of the aeroelastic system, can be examined by the nature of the Hopf bifurcation [12] of the associated nonlinear aerothermoelastic system [11, 13-14]. In the aerothermoelastic governing equations, the various nonlinear effects will be incorporated. This paper also shows the combined nonlinear effects of plunge-pitch freeplay on a typical section model. The combined plunge-pitch freeplay can usually be observed in an advanced generic missile pin that could be folded at its settled position [10]. A multi-purpose military missile fin with folded mechanism may have two-axial nonlinearities at the folding fin axis and pitch control axis, as shown in Fig. 1. This paper has considered an equivalent typical section model with 2-DOF motion with freeplay nonlinearity in both plunge and pitch directions, as shown in Fig. 2. The unsteady aerodynamic forces on the airfoil are evaluated by using the third order piston theory aerodynamics (PTA), and the resulting aeroelastic

equations are integrated numerically to give out the aeroelastic time responses of the airfoil motion and to show the dynamic instability.

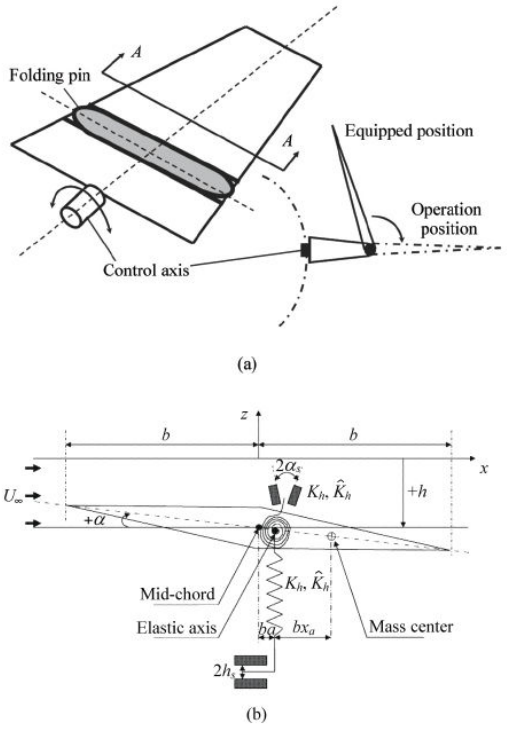

Fig. 1. Typical Section Model.

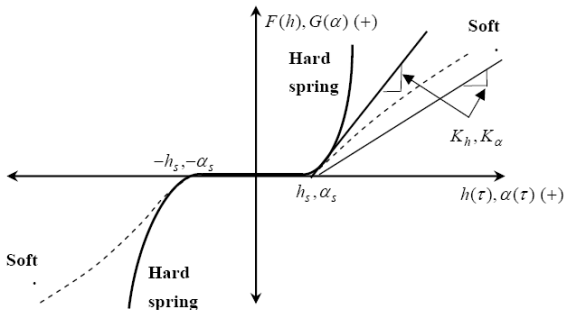

Fig. 2. Freeplay Nonlinear Plunge and Pitch Stiffness.

2. Nonlinear Aerothermoelastic Model

2.1. Nonlinear structural model

The structural model considered here is double-wedge 2-DOF plunging/ pitching airfoil. The model is free to rotate in the *x*-*z* plane and free to translate in the

vertical direction as shown in Fig. 1. The nonlinear restoring force and moment from bending and torsional springs for possible freeplay in both degrees-of-freedom have been considered. The nonlinear aerothermoelastic governing equations can be written as

$$m\ddot{h} + S_\alpha \ddot{\alpha} + c_h \dot{h} + F(h) = -L(t) \tag{1}$$

$$S_\alpha \ddot{h} + I_\alpha \ddot{\alpha} + c_\alpha \dot{\alpha} + G(\alpha) = M_{EA}(t) \tag{2}$$

The cubic stiffness functions (restoring force/moment) [10, 11, 15] (see Fig. 2) can be written as follows:

$$F(h) = F_a + F_b + F_c \;;\; G(\alpha) = G_a + G_b + G_c \tag{3}$$

$$F_a(h) = (K_h h; 0; K_h h)\; F_b(h) = (-K_h h_s; 0; K_h h_s)$$

$$F_c(h) = [\hat{K}_h (h - h_s)^3; 0; \hat{K}_h (h + h_s)^3] \tag{4}$$

for $(h > h_s; -h_s \le h \le h_s; h < -h_s)$.

Similar expressions for G_a, G_b and G_c can be expressed replacing the plunging variable h with the pitching variable α.

2.2. Effective torsional stiffness

The minimum value of the effective torsional rigidity stiffness (loss in the torsional rigidity) of instantaneously accelerated, double-wedge solid wings of constant chord and finite span subjected to axial stresses induced by aerodynamic heating is [16]:

$$(GJ_{eff} / GJ)_{\min} = 1 - 0.0456(E\alpha_{th} / G)\{[T_{aw}^{(f)} - T_{aw}^{(0)}] / \hat{\tau}^2\}. \tag{5}$$

where GJ and GJ_{eff} are the torsional rigidity at the room temperature and the effective (apparent) torsional rigidity accounting also for the additional torsional rigidity due to aerodynamic heating, respectively. In Eq. (5) E and G are the modulus of elasticity and torsional rigidity, respectively; $\hat{\tau}$ is the airfoil thickness ratio, $T_{aw}^{(0)}$ is the initial airfoil temperature at $t = 0$ (initial flight Mach number $M_\infty^{(0)}$), $T_{aw}^{(f)}$ is the final temperature for $t > 0$ (final flight Mach number $M_\infty^{(f)}$) and α_{th} is the linear coefficient of thermal expansion. In general, the adiabatic wall temperature (the concept of adiabatic wall temperature is used in the field of high velocity aerodynamics) is given by:

$$T_{aw} = T_\infty \{1 + [r(\gamma - 1)M_\infty^2 / 2]\} \tag{6}$$

Where γ is the isentropic gas coefficient, (γ= 1.4 for dry air), T_∞ is the free stream temperature at flight altitude and r is the temperature-recovery factor and in the case of a turbulent boundary layer on a plate, $r = \sqrt[3]{\text{Pr}}$ for Prandtl numbers Pr close to 1.

Substitution Eq. (6) into Eq. (5) with $r \approx 0.9$ and γ =1.4, the minimum torsional rigidity is:

$$(GJ_{eff}/GJ)_{\min} = 1-(0.00821)(E\alpha_{th}/G)T_{\infty}\{[M^{2^{(f)}}_{\infty} - M^{2^{(0)}}_{\infty}]/\hat{\tau}^2\} \tag{7}$$

implying that the maximum reduction (in per cent) in torsional stiffness depend on: (a) material $(E\alpha_{th}/G)$; (b) geometry ($\hat{\tau}$); (c) altitude (T_{∞}); and (d) velocity ($M^{2^{(f)}}_{\infty} - M^{2^{(0)}}_{\infty}$). Notice that the minimum torsional rigidity is independent of the magnitude of the heat-transfer coefficient. The torsional frequency of cantilevered beam can be written, including the loss in the effective torsional stiffness, as follows:

$$\omega_{\alpha} = (\pi/2L)\sqrt{[(GJ_{eff}/GJ)_{\min} GJ]/I_{\alpha}} \tag{8}$$

Herein, L represents the beam length and I_{α} is the mass polar moment of inertia per unit length.

2.3. Nonlinear piston theory aerodynamics (PTA)

To study the behavior of the nonlinear aeroelastic system in supersonic/hypersonic aeroelastic analyses, a third order expansion form of the piston theory aerodynamics (PTA) [17] model is used:

$$\frac{p(x,t)}{p_{\infty}} = 1+\gamma(\frac{v_z}{c_{\infty}}\eta)+\frac{\gamma(\gamma+1)}{4}(\frac{v_z}{c_{\infty}}\eta)^2+\frac{\gamma(\gamma+1)}{12}(\frac{v_z}{c_{\infty}}\eta)^3 \tag{9}$$

Eq. (9) can be used for low supersonic/hypersonic speed ($M_{\infty} \geq 1.3$) and for moderate angles-of-attack ($\alpha \leq \pm$ 20 deg). In Eq. (9) the local transverse velocity (downwash velocity) v_z normal to the airfoil surface may be expressed for upper and lower airfoil surface as follows [18, 19]:

$$\begin{aligned} v_{z,u} &= -\{\dot{h}+(x-ba)\dot{\alpha}\}+U_{\infty}\{-\alpha+\partial f_u(x)/\partial x\} \\ v_{z,l} &= \{\dot{h}+(x-ba)\dot{\alpha}\}-U_{\infty}\{-\alpha+\partial f_l(x)/\partial x\} \end{aligned} \tag{10}$$

$$\partial f_u(x)/\partial x = \hat{\tau} \text{ for } -b<x<0 \;;\; \partial f_u(x)/\partial x = -\hat{\tau} \text{ for } 0<x<b$$

$$\partial f_l(x)/\partial x = -\hat{\tau} \text{ for } -b<x<0 \;;\; \partial f_l(x)/\partial x = \hat{\tau} \text{ for } 0<x<b$$

2.4. Nonlinear aeroelastic governing equations

In dimensionless form, the system of governing equations of the 2-DOF double-wedge airfoil, elastically constrained by a nonlinear translational and torsional springs can be described as:

$$\xi''(\tau)+\chi_{\alpha}\alpha''(\tau)+2\zeta_h(\overline{\omega}/U^*)\xi'(\tau)+(\overline{\omega}/U^*)^2\overline{F}_a(\xi)\xi(\tau)+(\overline{\omega}/U^*)^2\overline{F}_b(\xi_s)+$$

$$(\overline{\omega}/U^*)^2 \overline{F}_c(\xi)[\xi^3(\tau) + 3(-1)^n \xi_s \xi^2(\tau) + 3\xi_s^2 \xi(\tau) + (-1)^n \xi_s^3] = \overline{L}(\tau) \tag{11a}$$

$$(\chi_\alpha / r_\alpha^2)\xi''(\tau) + \alpha''(\tau) + (2\zeta_\alpha / U^*)\alpha'(\tau) + (1/U^{*2})\overline{G}_a(\alpha)\alpha(\tau) + (1/U^{*2})\overline{G}_b(\alpha_s) +$$
$$(1/U^{*2})\overline{G}_c(\alpha)[\alpha^3(\tau) + 3(-1)^n \alpha_s \alpha^2(\tau) + 3\alpha_s^2 \alpha(\tau) + (-1)^n \alpha_s^3] = \overline{M}_{EA}(\tau) \tag{11b}$$

where

$$\overline{F}_a(\xi) = (1;0;1);\ \overline{F}_b(\xi) = (-\xi_s;0;\xi_s);\ \overline{F}_c(\xi) = (\hat{\eta}_h;0;\hat{\eta}_h)$$
$$\text{for } (\xi(\tau) > \xi_s, n = 1; -\xi_s \le \xi(\tau) \le \xi_s; \xi(\tau) < -\xi_s, n = 2) \tag{12}$$

Similar expressions for $\overline{G}'s$ can be obtained by replacing $\xi(\tau) \Leftrightarrow \alpha(\tau)$.

The unsteady aerodynamic lift and moment appearing in Eqs. (11) can be expressed as:

$$\overline{L}(\tau) = -\frac{\eta}{12M_\infty \mu}[12(\xi' - a\alpha' + \alpha) - 3(\gamma+1)\hat{\tau}\eta M_\infty(\alpha') +$$
$$M_\infty^2(\gamma+1)\eta^2(\xi' - a\alpha' + \alpha)((\xi' - a\alpha' + \alpha)^2 + 3\hat{\tau}^2 + (\alpha')^2)] \tag{13a}$$

$$\overline{M}_{EA}(\tau) = \frac{\eta}{12\mu M_\infty r_\alpha^2}[12(a\xi' - (1/3 + a^2)\alpha' + a\alpha) + 3(\gamma+1)\hat{\tau}\eta M_\infty(\xi' - 2a\alpha' + \alpha) -$$
$$M_\infty^2(\gamma+1)\eta^2(1/5(\alpha')^3 - a(\xi' - a\alpha' + \alpha)[(\xi' - a\alpha' + \alpha)^2 + 3\hat{\tau}^2] +$$
$$\alpha'[(\xi' - a\alpha' + \alpha)^2 + \hat{\tau}^2 - a\alpha'(\xi' - a\alpha' + \alpha)])] \tag{13b}$$

3. Time Domain Analysis

Flutter and post flutter analyses are complicated due to the presence of nonlinearities which are also sources of coupling. The lifting surface may exhibit equilibrium, periodic, or limit cycle to quasi-periodic motion depending on this coupling as well as the order of the nonlinearities. Also in certain regions of the parameter space the quasi-periodic behavior changes to a chaotic one depending on the geometrical parameters as well as initial conditions of the aeroelastic system. Because chaotic vibrations have no steady-state periodic solution, a direct numerical integration of the aeroelastic governing equation has been carried out. For this purpose Eqs. (11) can be written in the following matrix form:

$$\mathbf{M}\mathbf{u}''(\tau) + \mathbf{C}\mathbf{u}'(\tau) + (\mathbf{KL} + \mathbf{KNL})\mathbf{u}(\tau) = (\mathbf{QL1_{ext}} + \mathbf{QNL1_{ext}})\mathbf{u}'(\tau) +$$
$$(\mathbf{QL2_{ext}} + \mathbf{QNL2_{ext}})\mathbf{u}(\tau) - \mathbf{Q_f} \tag{14}$$

The aerodynamic dampening and stiffening matrices $\mathbf{QNL1_{ext}}$ and $\mathbf{QNL2_{ext}}$ in Eq. (14) contain both uncoupling and coupling nonlinear quadratic and cubic terms, respectively. The matrices $\mathbf{QL1_{ext}}$ and $\mathbf{QL2_{ext}}$ include the dampening and stiffening aerodynamic linear terms, respectively. To perform the nonlinear aeroelastic

analysis in the time domain, Eq. (14) is converted into a system of first order ODEs in state

$$\dot{\mathbf{y}} = \mathrm{A}\,\mathbf{y} + \mathrm{B}\,\mathbf{u} \tag{15}$$

4. Numerical Simulation, Discussion and Conclusions

To emphasize the importance of aerodynamic heating on the nonlinear aerothermoelastic behavior of the examined aeroelastic system in the presence of an initial structural freeplay, the influence of the loss in effective torsional stiffness of a solid thin double-wedge wing has been analyzed. A number of bifurcation diagrams were constructed from the response amplitude as a function of the flight Mach number, Fig. 3. The geometric and flow parameters, initial conditions and the freeplay magnitudes are presented in Table 1.

Table 1. Baseline Parameters.

2-DOF Plunging-Pitching Airfoil	
Material	Titanium (Ti-6%Al-4%V), ρ = 4420 kg/m^3 TEC (0-100^{o}C) 8.8×10^{-6}/K, TEC (0-300^{o}C) 9.2×10^{-6}/K E=114×10^9 N/m^2, G=43.51×10^9 N/m^2, ϑ=0.31
Flight condition	H=5000; 10000 m, ρ_∞=0.736; 0.4135 kg/m^3 c_∞=317.07; 299.53 m/s T_∞=255.7; 223.26 K, η=1, γ=1.4
Airfoil geometry parameters	Rectangular shape, AR = 4.5, b = 0.25 m , $\hat{\tau}$=0.05; 0.1, m=55.2 kg
Airfoil physical parameters	χ_α=0.25, r_α=0.5, ζ_h, ζ_α = 0, a=-0.25
Cubic stiffening	$\hat{\eta}_h, \hat{\eta}_\alpha$=0; 20
Initial condition	$\xi(\tau = 0) = \dot{\xi}(\tau = 0) = \dot{\alpha}(\tau = 0) = 0$, $\alpha(\tau = 0) = 5$ deg
Initial freeplay	α_s = 1 deg , ξ_s = 0.01

Three cases were performed to demonstrate the complex nonlinear behaviors of the system. Case #1 is for a system with no aerodynamic heating and ($\hat{\eta}_h = \hat{\eta}_\alpha = 0$), such that M_{LF} = 15.2 (LF, linear flutter). Case # 2, is for the system with aerodynamic heating and $\hat{\eta}_h = \hat{\eta}_\alpha = 0$ yielding M_{LF} = 10.4. Because of symmetric pitch LCO amplitude and to have a better graphical representation, only the positive side of the LCO curve is presented for Case #2. Case # 3 is for a system with aerodynamic heating and ($\hat{\eta}_h = 0$, $\hat{\eta}_\alpha = 20$) and the flutter speed is the same as case #2. For this case, the negative side of the pitch LCO is displayed for clarity. Note that the simulations are restricted to cases where the pitching displacement is

within ±20 deg to remain within the limits of validity of the proposed model and approach. In Fig. 3a, where the altitude is 10000 m and $\hat{\tau} = 0.1$, the aeroelastic system exhibit a bifurcation behavior for all three cases at $M_\infty \approx 1.5$ due to the presence of coupling freeplays (in both plunge and pitch). For the speed range $(1.5 < M_\infty \leq 7)$, different types of response behavior (periodic, quasi-periodic or chaotic) will occur. Within the speed ranges $(7 < M_\infty \leq 14)$ for Case #1, $(7 < M_\infty \leq 10)$ for Case #2, and $(7 < M_\infty \leq 11)$ for Case #3, a stable LCO is experienced; its amplitude increases with the increase of the flight Mach number. From Fig. 3a it appears that pitch LCO amplitude for Case #1 is less than 12 deg for speed less than the linear flutter speed. When considering Case #2, the pitch amplitude is about 10 deg at $M_\infty \approx 10$, while if the pitching stiffness nonlinearity is considered, Case #3, the pitch amplitude reaches 10 deg at $M_\infty \approx 11$. This result reveals that the flutter speed as well as the LCO behavior is affected by the loss of the torsional stiffness. The effect of varying the thickness ratio is indicated in Fig. 3b. Herein, the altitude is 10000 m and $\hat{\tau} = 0.05$. A stable LCO is experienced for all three cases. Although the system accounts for freeplays, no chaotic behavior is encountered. Decreasing the thickness ratio has a significant effect on the linear flutter value. This fact is evident in Fig. 3b where $M_{\mathrm{LF}} = 7.2$ for the same Case #1 of Fig. 3a but with a smaller thickness ratio.

In addition, the linear flutter for Cases #2 and #3 decreases to $M_{\mathrm{LF}} = 4.8$. Although in Case #3 the pitching stiffness nonlinearity is considered and contributes to decrease the amplitude of the LCO as compared to Case # 2 (compare the value of the pitching LCO amplitude at $M_\infty \approx 5.5$), there is certainly a detrimental reduction in flutter speed as well as the amplitude of the LCO as compared to the corresponding Cases #2 and #3 of Fig. 3a. Results for a flight altitude of 5000 m are also presented in Fig. 3c. The three cases present a different behavior: $(1.5 < M_\infty \leq 3)$ (periodic LCO), $(3 < M_\infty \leq 4)$ (stable LCO), $(4 < M_\infty \leq 5)$ (chaotic behavior) for all three cases. For $M_\infty > 5$, Case #1, $(5 < M_\infty \leq 10)$ (stable LCO, $M_{\mathrm{LF}} = 10.6$), Case #2 (that is when accounting for the influence of aerodynamic heating) $(5 < M_\infty \leq 8)$ (stable LCO, $M_{\mathrm{LF}} = 8.3$), Case #3 (that is accounting for both aerodynamic heating and pitch stiffening nonlinearity), $(5 < M_\infty \leq 10)$, (stable LCO, $M_{\mathrm{LF}} = 8.3$). In Fig. 4 the curves show how susceptible this system is to loss of torsional stiffness when aerodynamic heating are considered in conjunction with altitude, thickness ratios. Curve #1 does not include the aerodynamic heating; therefore there is no reduction in the effective torsional stiffness. It appears that for a flight Mach number $M_\infty \approx 4$, Curves #2 (10000 m and $\hat{\tau} = 0.1$), #4 (5000 m and $\hat{\tau} = 0.1$) and #3 (10000 m and $\hat{\tau} = 0.05$) present a reduction in torsional stiffness of 5%, 7%, and 25% of the original value. Clearly the thickness ratio has a more detrimental role in the loss in torsional stiffness and consequently in the flutter speed and the LCO behavior of the examined aeroelastic lifting surface.

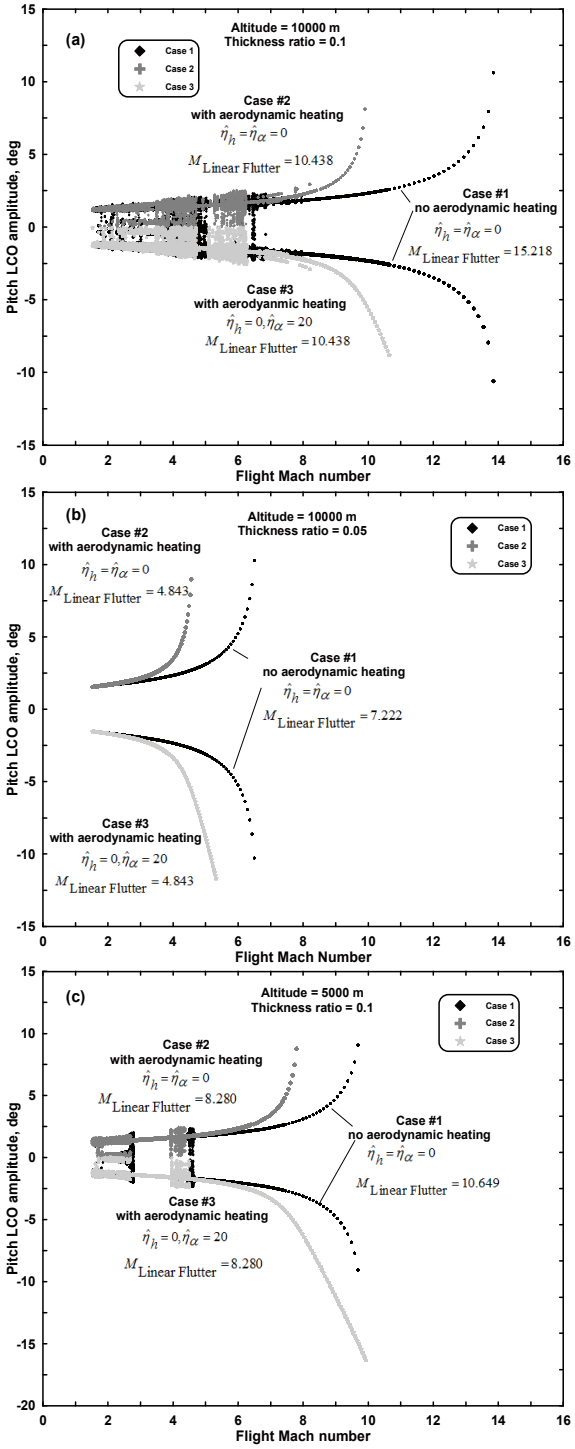

Fig. 3. Bifurcation Pitch Diagrams.

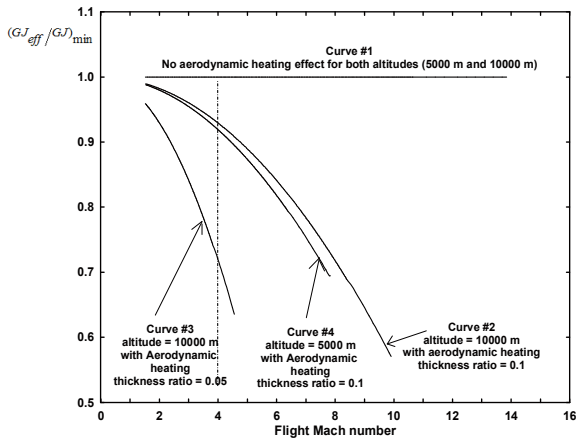

Fig. 4. Reduction in Torsional Stiffness for Solid Double-wedge Wing due to Aerodynamic Heating, Effect of Thickness Ratio, and Altitude

References

1. Marzocca P., Librescu L., Chiocchia G. (2002). Aeroelastic response of 2-D lifting surfaces to gust and arbitrary explosive loading signatures. *Int. J. Impact Engineering*, Vol. 25, No. 1, 41-65.
2. Marzocca P., Librescu L., Silva W.A. (2002). Aeroelastic response of nonlinear wing section by functional series technique. *AIAA J.*, Vol. 40, No. 5, 813-824.
3. Marzocca P., Librescu L., Silva W.A. (2002). Flutter, post-flutter and control of a supersonic 2-D lifting surface. *J. Guidance, Control, and Dynamics*, Vol. 25, No. 5, 962-970.
4. Librescu L., Marzocca P., Silva W.A. (2002). Post-flutter instability of a shell type structures in hypersonic flow field. *J. Spacecraft and Rockets*, Vol. 39, No. 5, 802-812.
5. Librescu L., Chiocchia G., Marzocca P. (2003). Implications of cubic physical/ aerodynamic nonlinearities on the character of the flutter instability boundary. *Int. J. Nonlinear Mechanics*, Vol. 38, No. 3, 173-199.
6. Laith K. Abbas, Chen Qian, Piergiovanni Marzocca, Gürdal Zafer, Abdalla Mostafa. (2008). Active aerothermoelastic control of hypersonic double-wedge lifting surface. *Chinese Journal of Aeronautics*, Vol. 21, No. 2, 8-18.
7. Librescu L., Na S., Marzocca P., et al. (2003). Active aeroelastic control of 2-D wing-flap systems in an incompressible flow field. *AIAA Paper*, 2003-1414.
8. Dowell E.H. (1978). *A modern course in aeroelasticity*. Sijthoff and Noordhoff, Rockville, MD.
9. Dowell E.H., Edwards J. and Strganac T. (2003). Nonlinear aeroelasticity. *J. Aircraft*, Vol. 40, No. 5, 857-874.
10. Hyun D.H., Lee I. (2000). Transonic and low-supersonic aeroelastic analysis of a two-degree-of-freedom airfoil with a freeplay nonlinearity. *J. Sound and Vibration*, Vol. 234, No. 5, 859-880.
11. Lee B.H.K., Price S.J. and Wong Y.S. (1999). Nonlinear aeroelastic analysis of airfoils: Bifurcation and chaos. *Progress in Aerospace Sciences*, Vol. 35, No. 3, 205-334.
12. Hopf, E. (1942). Bifurcation of a periodic solution from a stationary solution of a system of differential equations. *Berlin Mathematische Physics Klasse, Sachsischen Akademic der Wissenschaften Leipzig*, Vol. 94, 3-32.

13. Holmes P.J. (1977). Bifurcations to divergence and flutter in flow-induced oscillations: A finite-dimensional analysis. *J. Sound and Vibration*, Vol. 53, No. 4, 471-503.
14. Mastroddi F., Morino L. (1996). Limit-cycle taming by nonlinear control with application to flutter. *Aeronautical J.*, Vol. 100, No. 999, 389-396.
15. Zhao, Y.H. and Hu, H.Y. (2004). Aeroelastic analysis of a nonlinear airfoil based on unsteady vortex lattice model. *J. Sound and Vibration*, Vol. 276, 491–510.
16. Budiansky, B. and Mayers, J. (1956). Influence of aerodynamic heating on the effective torsional stiffness of thin wings. *J. Aeronautical Sciences*, Vol. 23, No. 12, 1081-1093 and 1108.
17. Librescu, L., Marzocca, P., and Silva, W.A. (2002). Supersonic/hypersonic flutter and post-flutter of geometrically imperfect circular cylindrical panels. *J. Spacecraft and Rockets,* Vol. 39, No. 5, 802–812.
18. Ashley H. and Zartarian G. (1956). Piston theory – a new aerodynamic tool for the aeroelastician. *J. Aerospace Sciences*, Vol. 23, No. 10, 1109–1118.
19. Thuruthimattam B.J., Friedmann P.P., McNamara J.J. and Powell K.G. (2002). Modeling approaches to hypersonic aeroelasticity. *ASME Paper* 2002-32943, New Orleans, Louisiana, USA.